An Investigation into a Sequential Port-Injection of Natural Gas in a Multi-Cylinder Turbocharged Diesel Dual Fuel Engine

Wanwisa Jantaradach[1], Orawan Wattanapanichaporn[1], Krisada Wannatong [2] and Tanet Aroonsrisopon[1,*]

[1] Department of Mechanical Engineering, Faculty of Engineering, Kasetsart University, 50 Phahonyothin Road, Chatuchak, Bangkok 10900, Thailand

[2] Energy Application Technique and Engine Test Department, PTT Research and Technology Institute, PTT Public Company Limited, 71 Moo 2, Phahonyothin Road, km. 78, Wangnoi, Ayutthaya 13170, Thailand

*E-mail: tanet.a@ku.ac.th

Abstract

Multi-point port fuel injections have been commonly used in conventional premixed charge engines. The current study investigated use of a sequential port injection of natural gas in a four-cylinder turbocharged diesel dual fuel engine. The engine was run under part-load steady-state conditions at 1200 rpm and 1800 rpm for a range of natural gas injection timings. CFD results were also presented to simulate flow characteristics around the intake ports.

Data showed the natural gas injection timings (referred to the end of injection, EOI) played an important role in the cylinder-to-cylinder variations in pressure traces and the cyclic variation of the combustion in each cylinder. The main reason for these combustion variations was found to be the variation of the mixture lambda between cylinders. The cylinder variation in mixture lambda was most likely depended on the amount of the natural gas left-over in the intake ports after intake valve close. This left-over natural gas portion was then drawn into other cylinders. The optimum EOI timing for minimizing both cyclic and cylinder variations was found to be at the exhaust TDC (around the IVO timing). Using the optimum EOI timing for DDF operations has a potential to achieve greater engine efficiency and lower HC, CO and NO_x engine-out emissions. The findings from the current study will facilitate the improvements of DDF engine operations.

Keywords*:* Natural gas; Port injection; Diesel dual fuel; Premixed charge; Cylinder-to-cylinder variations.

1. Introduction

Natural gas (NG) has been recognized as one of the promising alternative fuels for internal combustion engines. With the ability to achieve a high compression, a compression-ignition engine can produce a higher efficiency than a spark-ignition engine. These reasons have drawn interest in investigating a diesel engine using high NG replacement ratios. In such a dual fuel engine, NG is served as a main fuel and diesel fuel is served as a pilot fuel. The term “diesel dual fuel (DDF)” engine is referred to as a premixed-natural-gas diesel-ignited engine in the current study.

In dual fuel engines, the main fuel is introduced either homogeneously by a mixer or port injectors in the intake system [1–7] or stratifically by a direct injection into the combustion chamber [8]. The pilot diesel fuel injection serving as an ignition source is usually injected during the compression stroke [1–9]. When converting a diesel engine to a dual fuel engine, the combustion chamber is normally remained unchanged and the compression ratio is therefore maintained on relatively high levels. A high auto-ignition resistance of the main fuel is desirable to avoid problems with knock.

The study by Czerwinski et al [10] converted a diesel engine to a natural gas dedicated engine using sequential port injection. They compared different gas injectors available on the market for steady-state and transient engine operations. It was found that the end of natural gas injection timing (EOI) influenced the variation in the air-fuel ratio between cylinders. The optimum EOI for reducing the cylinder-to-cylinder variation in combustion processes changed with engine operating conditions.

The focus of this study was to investigate the effects of gas injection timing on cylinder-to-cylinder variations in the cylinder outputs and, ultimately, survey for the optimum gas injection

timing for low-speed DDF operations. The findings from the current study will facilitate the improvements of DDF engine operations.

2. Experimental Setup

2.1 Test bed setup

All experiments were performed at PTT Research and Technology Institute. The latest version of a VN turbocharged Toyota 2KD-FTV diesel engine was used in the current research. Engine specifications are shown in Table 1.

Table. 1 Engine specifications

# Cylinder	4 cylinders, inline
Displaced volume	2,494 cc
Stroke	93.8 mm
Bore	92 mm
Connecting rod	158.5 mm
Compression ratio	17.4:1
Number of valves	16 valves (DOHC)
Exhaust valve open	30° bBDC
Exhaust valve close	0° bTDC
Inlet valve open	2° bTDC
Inlet valve close	31° aBDC

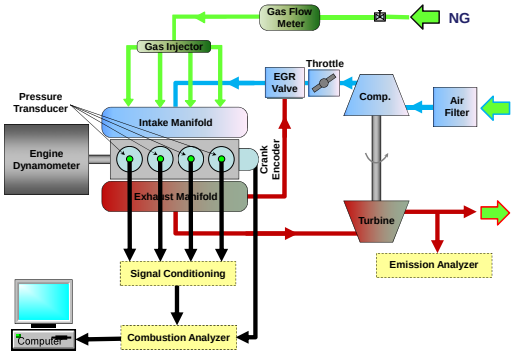

Fig. 1 Schematic of the experimental setup

Fig. 1 shows a schematic of the experimental setup used in the current study. The engine was coupled to a DC dynamometer. The air at a room condition was drawn to the intake system. Natural gas was supplied via a sequential port injection system similar to our previous work [9]. Each natural gas injector for each cylinder was connected with a rubber hose and attached to the intake runner, which have the total length of approximately 345 mm, from the injector tip to the inlet valves. Cylinder pressure data of 150 consecutive cycles from all cylinders were recorded for combustion data analysis. For each cycle, the crank angle resolution of pressure data of 0.2° was recorded. The coolant temperature was maintained at 85°C. The oil temperature was maintained at 90°C. Four wide-band lambda probes were installed at the spacer attached between the exhaust ports and the exhaust manifold to measure exhaust A/F of each cylinder. Exhaust gas emissions were analyzed by using the Horiba MEXA 7100 DEGR gas analyzer. Data of smoke emissions were not available to present in this paper. Although smoke is one of the major common emissions from conventional diesel engines, it was found in our previous study [9] that acceptable DDF combustion produced much less smoke than conventional diesel combustion.

2.2 Fuels

The properties of diesel fuel and natural gas in this study are shown in Tables 2 and 3.

Table 2 Properties of natural gas used in the current study.

Methane number	83
Wobbe index, MJ/m^3	40.5
Higher heating valve, MJ/kg	37.71
Lower heating valve, MJ/kg	34.1
Stoichiometric A/F	11.68
MW, kg/kmole	22.39
Methane, % by mole	74.2
Ethane, % by mole	5.8
Propane, % by mole	2.3
n-Butane, % by mole	0.4
i-Butane, % by mole	0.5
Larger hydrocarbons (> C6), % by mole	0.3
CO_2, % by mole	14.5†
N_2, % by mole	2

Table 3 Properties of diesel fuel (B3) used in the current study.

Density, kg/m^3 (calc.)	0.83
Higher heating valve, MJ/kg (calc.)	45.64
Lower heating valve, MJ/kg (calc.)	42.75
Stoichiometric A/F (est.)	14.41
MW, kg/kmole (est.)	170
C (est.)	12.3
H (est.)	21.92
O (est.)	0.04

2.3 Test matrices

The engine conditions were selected from driving conditions frequently used in the New European Driving Cycle (NEDC) based on the chassis dynamometer test using the Toyota 2KD-FTV engine [9]. In this study, we explored

steady-state DDF operations at lower engine speeds, 1200 and 1800 rpm to observe the effects of gas injection timing on the engine operation. Experimental conditions are provided in Table 4.

Table 4 Experimental matrices

No.	mode	Speed	Diesel	NG	NG_EOI
		[rpm]	[mg/cyc]	[mg/cyc]	[bTDC]
1.	DDF	1200	2.99	10.97	450° to 180°
2.	DDF	1800	2.99	10.97	450° to 180°

Under these conditions, the energy input was kept constant where the amount of each diesel and natural gas supplied per cycle was the same for all conditions. The gas injection timing defined by the end of injection (EOI) was varied from 450º to 180º before firing TDC (i.e. from 90º before to 180º after exhaust TDC). For all engine conditions, diesel fuel was supplied through each injector using the single-pulse injection technique like our previous study [9]. In this study, the start of diesel injection (SOI) timing was kept constant at 33º bTDC for 1200 rpm and at 38º bTDC for 1800 rpm. The rail pressure for each DDF operation was set at the same pressure as for the OEM diesel operations under the same load. For each data point, the injection signal for each individual fuel injector (for both NG and diesel) was controlled independently to minimize the deviation of injected mass between injectors.

3. Result and Discussion

3.1 Effect of gas injection timing on combustion characteristics

Fig. 2 shows the brake torque for different gas injection timings and engine speeds. It appeared that with the gas injection timing around exhaust TDC, the brake torque reached its maximum value for each engine speed. One could notice that for the same input energy supplied per cycle, the brake torque of the lower engine speed was greater than that of the higher speed. The reduction of brake torque found with higher engine speed was due to greater friction. Data for the brake engine efficiency for both engine speeds are presented in Fig. 3. Note that a change in the brake torque correlated with a change in the engine efficiency as the input energy was kept constant.

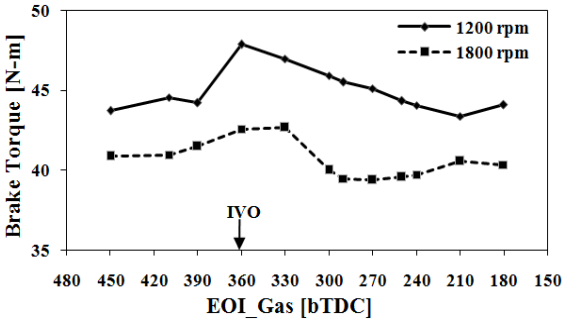

Fig. 2 Brake torque for different gas injection timings at 1200 and 1800 rpm.

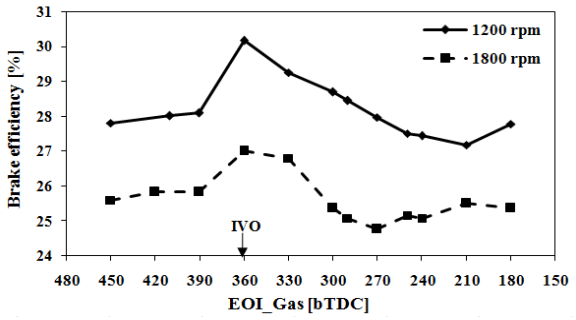

Fig. 3 Brake engine efficiency for different gas injection timings at 1200 and 1800 rpm

Fig. 4, 5 and 6 show phenomena in each combustion chamber. The COV of IMEPn for each cylinder representing the "cyclic variation" in combustion was calculated from in-cylinder pressure data over 150 consecutive engine cycles. The output variation from cylinder to cylinder (termed by "IMEPn variation") was defined by the coefficient of variation in the averaged value of IMEPn in each cylinder. It was found that IMEPn, its COV and its cylinder-to-cylinder variation for both engine speeds followed the same trend. At the engine speed of 1200 rpm, retarding EOI from 450º to 360º bTDC decreased the cylinder variation. At 360º bTDC, the brake torque and the brake efficiency both reached their maximum values. As the gas injection timing continued to retard from this point, the cylinder variation slightly increased until EOI = 250º bTDC where the cylinder variation increased rapidly. A similar trend was found at 1800 rpm, where the EOI timing for minimizing the cylinder variation slightly shifted to 390º bTDC. Although this timing produced lowest cylinder variation, the optimum timing for best DDF operation was chosen at 360º bTDC (thus, around the IVO timing) due to greater engine efficiency with only small increase in cylinder variation. With these optimum gas injection timings, we could also achieve the lowest cyclic variation (i.e. COV of IMEPn) for all cylinders. It was also found that the combustion in cylinder 4 was most sensitive to changes in the EOI timing.

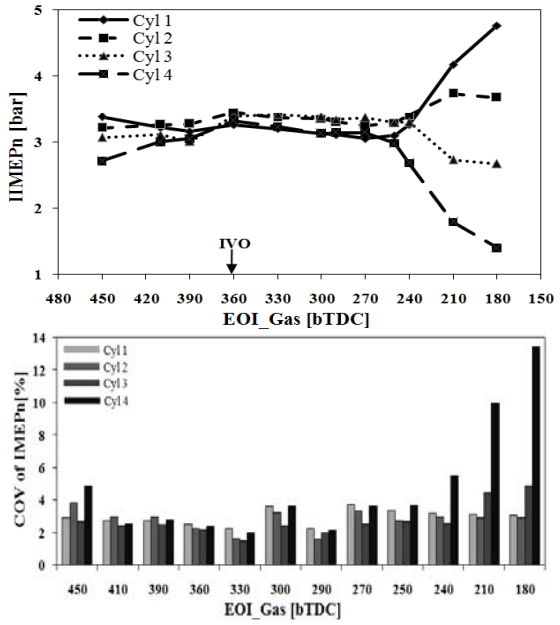

Fig. 4 IMEPn and its COV for each cylinder at different EOI timings at 1200 rpm (the horizontal scale in the bottom graph is not linear).

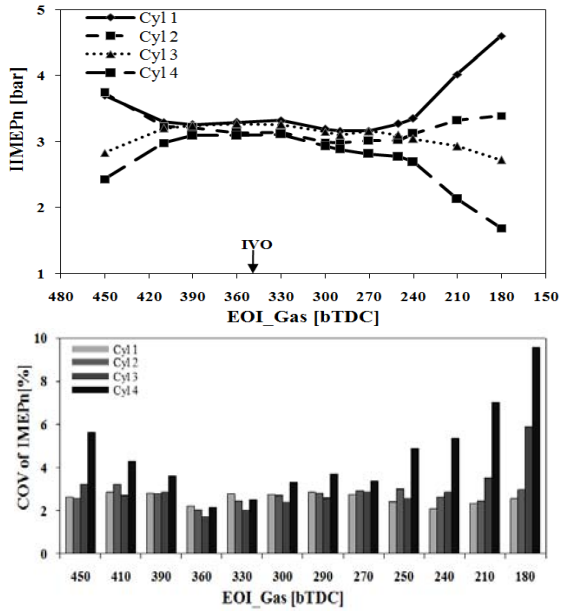

Fig. 5 IMEPn and its COV for each cylinder at different EOI timings at 1800 rpm (the horizontal scale in the bottom graph is not linear).

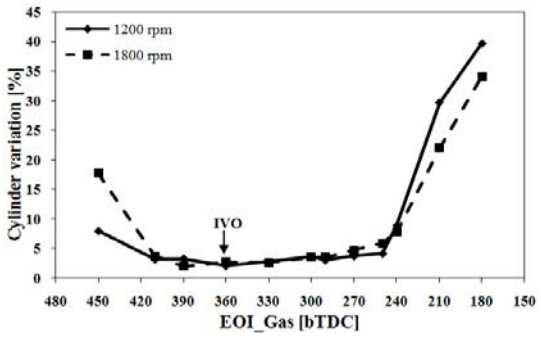

Fig. 6 Cylinder variation for different gas injection timings at 1200 and 1800 rpm

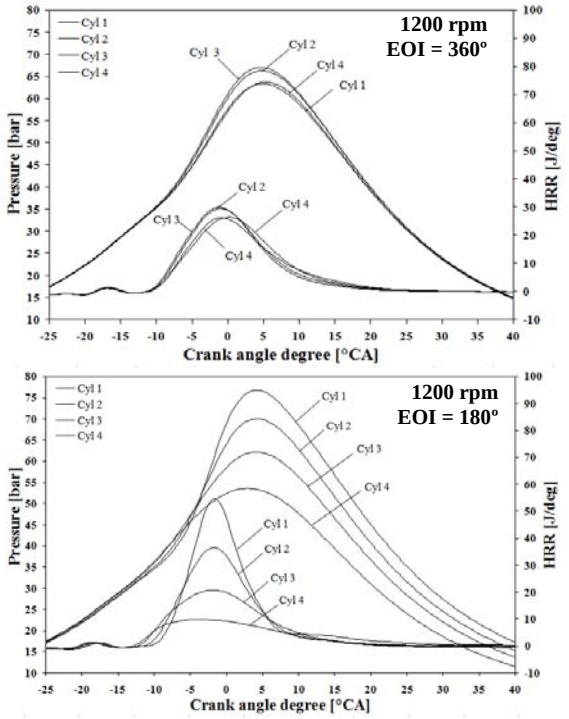

Fig. 7 Cylinder pressure and heat release rates for the EOI timings of 360° bTDC (top) and 180° bTDC (bottom) at 1200 rpm

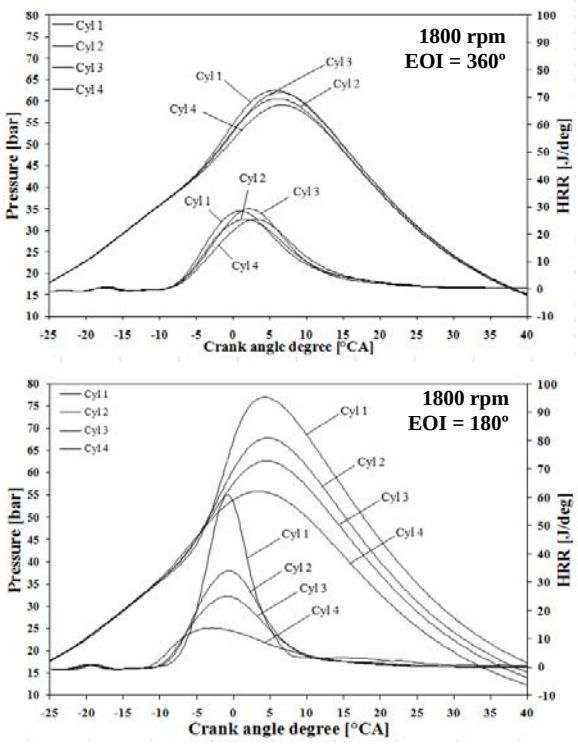

Fig. 8 Cylinder pressure and heat release rates for the EOI timings of 360° bTDC (top) and 180° bTDC (bottom) at 1800 rpm

Fig. 7 and Fig. 8 show in-cylinder pressure histories and heat release rates for engine conditions at 1200 and 1800 rpm, respectively. As one would expect, with the optimum EOI

timing, the pressure and heat release rates each was nearly overlaid for all cylinders. This also confirmed that we had a very similar and repeatable amount of injected mass from each fuel injector as we expected. With the EOI of 180° bTDC, as an example of a poor timing, the pressure and heat release data from cylinder to cylinder showed a large deviation. At this EOI timing, cylinder 1 showed the greatest energy release from combustion, in contrast, with cylinder 4 showing the smallest. From these observations, we hypothesized that with the diesel mass trapped being the same for all cylinders, the amount of natural gas trapped in each cylinder after IVC would be the main factor responsible for the cylinder variation as the EOI was varied.

3.2 Effect of gas injection timing on emission characteristics

Retarding the EOI timings from 450° to 360° caused CO to decrease with THC (also CH_4) being nearly unchanged. As the EOI was retarded from 360° to 270°, it appeared a clear trend that CO, THC, and CH_4 all increased. By comparisons, the greater amounts of these incomplete combustion products in this EOI range corresponded to a cooler EGR temperature (Fig. 9), a slightly lower intake manifold temperature (Fig. 10), a greater cylic variation (Fig. 4 and 5) and a larger cylinder variation (Fig. 6) in the combusiton processes. As the EOI continuted to retard from 270° to 180° bTDC, the engine-out hydrocarbon emissions tended to decrease. This corresponded to the hotter EGR temperature which was mainly due to stronger combustion in cylinder 1 and cylinder 2 (Fig.7 and 8). This then preheated the intake air and resulted in the hotter manifold temperature. The hotter intake temperature also promoted the combustion in cylinder 1 and cylinder 2, which then resulted in greater NO_x as previously discussed. As for CO, it appeared the opposite trend to that of HC at 1200 rpm, but nearly unchanged at 1800 rpm. This subtle trend was a result from combined effects including the hotter intake temperature, the greater cyclic variation and the greater cylinder-to-cylinder diviation in the combustion processes.

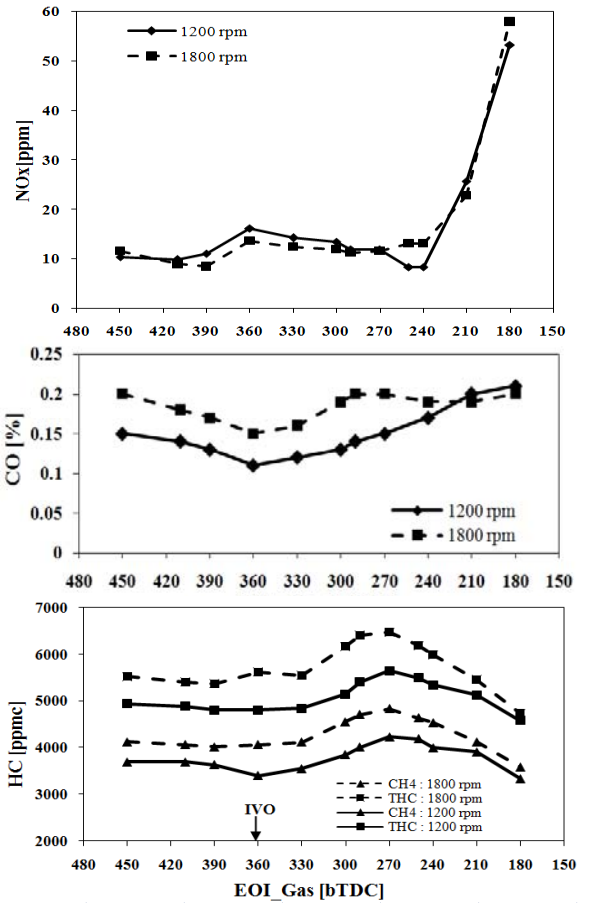

Fig. 8 NO_x, CO, total hydrocarbon (THC) and methane engine-out emissions for different gas injection timings.

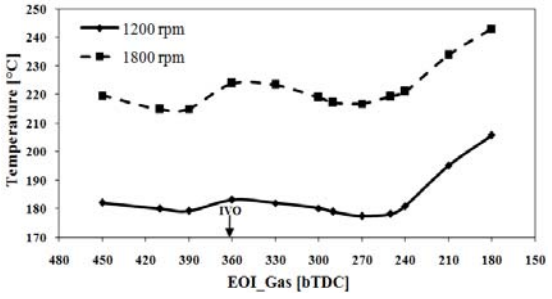

Fig. 9 EGR temperatures for different gas injection timings.

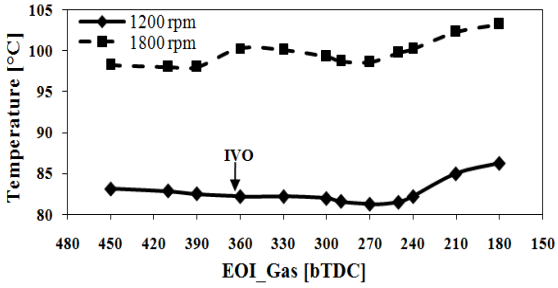

Fig. 10 Intake manifold temperatures for different gas injection timings.

3.3 Discussion of cylinder-to-cylinder variation

To gain a better insight into the cylinder-to-cylinder variation in the combustion, one can look at the measured lambda at each cylinder exit in Fig. 11 and 12, presented for the engine speeds of 1200 rpm and 1800 rpm, respectively. In each graph, the measured lambda from each cylinder is displayed with clustered bars and the cylinder-to-cylinder variation in the lambda (termed by the "lambda variation") is displayed with the dotted line. The lambda variation was defined by the coefficient of variation in the measured lambda in each cylinder. Note that the horizontal axis in each figure is not plotted on a linear scale.

We had the fifth lambda probe installed at the exhaust manifold. This gave us the total exhaust lambda being 1.65 at 1200 rpm and 1.54 at 1800 rpm. As the lambda variation between cylinders grew, it appeared a trend that cylinder 4 had the leanest charge, followed by cylinder 3 that had leaner mixtures than the averaged values for both engine speeds. Cylinder 1 and cylinder 2 had less lean mixtures than the averaged engine-out lambda values.

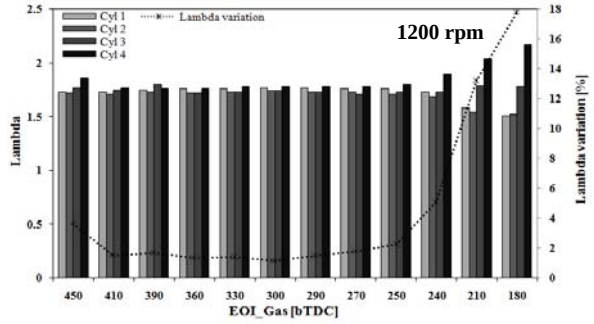

Fig. 11 Measured exhaust lambda at each cylinder exit (clustered bars) and its variation between cylinders (dotted line) for different gas injection timings at 1200 rpm.

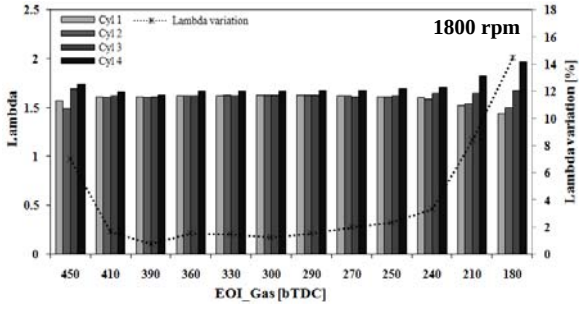

Fig. 12 Measured exhaust lambda at each cylinder exit (clustered bars) and its variation between cylinders (dotted line) for different gas injection timings at 1800 rpm.

Based on the observations, the cylinder-to-cylinder variation in exhaust lambda was found to be trend wise with the cylinder variation in the IMEP as shown in Fig. 13 and 14. This agreement of the data was not unexpected. Lambda can be linked with the amount of the input energy trapped in each cylinder and the IMEP represents the output work. If the cylinder-to-cylinder variation in the input energy is large, one would expect to observe a large cylinder variation in the output.

It should be noted that the cylinder-to-cylinder variation in the IMEP of diesel dual fuel operations can involve several factors other than the variation in NG trapped in each cylinder including the variation of air trapped, the variation of EGR ratio in the charge, the variation in diesel mass between injectors, the variation in intake port temperatures, and so on. For more detailed investigation of cylinder-to-cylinder variations in DDF combustion, one can refer to the other literature of our research work on this engine [11].

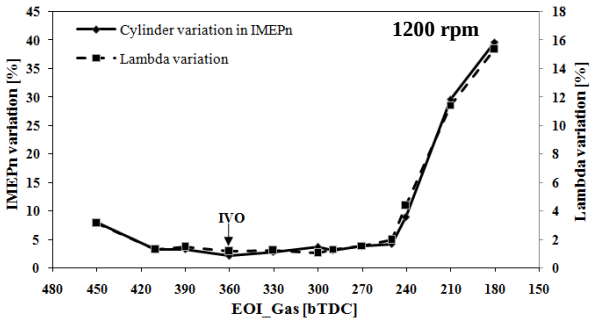

Fig. 13 A comparison between cylinder-to-cylinder variations in the net IMEP (solid line) and the exhaust lambda (dash line) for different gas injection timings at 1200 rpm.

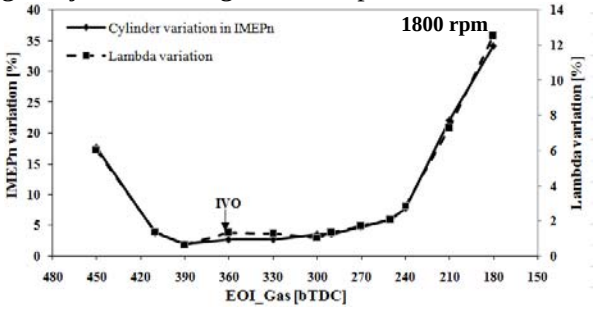

Fig. 14 A comparison between cylinder-to-cylinder variations in the net IMEP (solid line) and the exhaust lambda (dash line) for different gas injection timings at 1800 rpm.

As an assessment to intake flow phenomena, we previously performed CFD simulations for this engine using the AVL-FIRE software

package to study effects of port-injection timings on intake flow behaviors and mixture distributions in the intake manifold [12]. Results indicated that the optimum gas injection timing helped reduce the amounts of natural gas trapped in the intake ports after IVC. These amounts of fuel were later drawn into the intake manifold and entered other cylinders as their intake valves opened. The greater the amounts of natural gas left over in the intake ports, the more potential could it produce greater cylinder-to-cylinder variation in the air-fuel ratio.

To provide more insights into the flow characteristics around the intake ports, we compare the two cases: the extremely worse timing, 90° after firing TDC (i.e. during the expansion stroke), and the better EOI timing, 270° before firing TDC (i.e. during the intake stroke), and as shown in Fig 13. At 270° before TDC, one can observe the motion of methane (a surrogate model for natural gas) being drawn towards the direction of the cylinder entrance. On the other hand, with the EOI of 90° after TDC, a large portion of methane jet impinges at the wall of the intake runners and accumulates in this area.

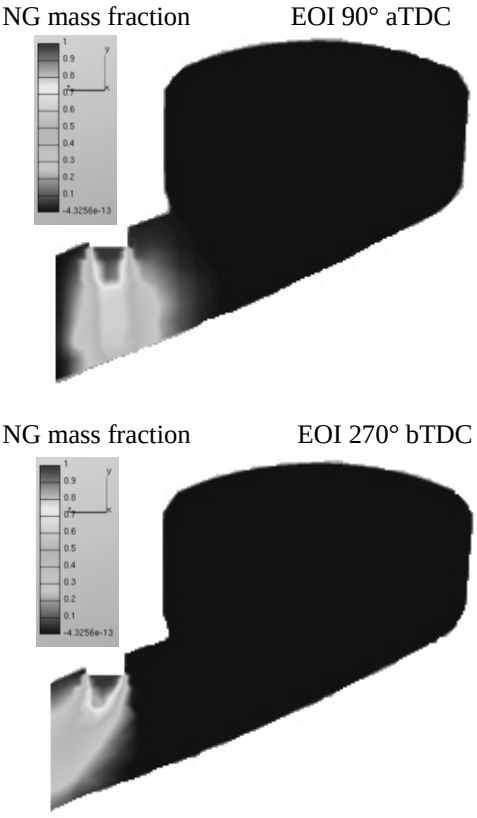

Fig.13 Predictions by AVL-FIRE simulations for natural gas flow characteristics around the intake runner at EOI = 90° after firing TDC (top) and 270° before firing TDC (bottom).

4. Conclusion

Data have been presented for multi-cylinder DDF operations using a sequential port-injection of natural gas. Experiments were conducted under steady-state DDF operation at 1200 and 1800 rpm for different gas injection timings. The conclusions can be drawn as follows:

- The EOI timing played an important role in both cyclic variation and cylinder variation in the cylinder outputs.
- As the EOI timing was varied, the main reason contributing to these variations in the IMEPn between cycles and cylinders was the variation in the mixture lambda between cylinders.
- The cylinder variation in mixture lambda was most likely depended on the amount of the natural gas left-over in the intake ports after intake valve close. This left-over natural gas portion was then drawn into other cylinders.
- The optimum EOI timing for minimizing both cyclic and cylinder variations was found to be at the exhaust TDC (around the IVO timing).
- Using the optimum EOI timing for DDF operations has a potential to achieve greater engine efficiency and lower HC, CO and NO_x engine-out emissions.

5. Acknowledgement

The authors would like to acknowledge the financial and technical support of PTT Public Company Limited (Thailand) and Kasetsart University (Thailand). We would like to thank Thananchai Tepimonrat for great assistance in laboratory work. Special thanks go to Sureeporn Sombut and Ekkawut Pattarajaree for the AVL-FIRE simulation results. We also acknowledge AVL LIST GmbH for granted use of AVL-FIRE under the university partnership program.

6. References

[1] Karim, G.A., Liu, Z., and Jones, W. (1993) Exhaust Emissions from Dual Fuel Engines at Light Load, SAE Technical Paper, No. 932822.
[2] Karim, G.A. (2000) Combustion in Gas Fuelled Compression-Ignition Engines, ASME ICE Fall Technical Conference.
[3] Singh, S., Krishnan, S.R., Srinivasan, K.K., and Midkiff, K.C. (2004) Effect of Pilot Injection Timing, Pilot Quantity and Intake Charge Conditions on Performance and Emissions for an Advanced Low-Pilot-Ignited Natural Gas Engine,

International Journal of Engine Research, Vol. 5, No. 4, JER 00404.
[4] Papagiannakis, R.G., and Hountalas, D.T. (2003) Experimental Investigation Concerning the Effect of Natural Gas Percentage on Performance and Emissions of a DI Dual Fuel Diesel Engine, Applied Thermal Engineering, Vol. 23, pp. 353-365.
[5] Papagiannakis, R.G., Hountalas, D.T., Rakopoulos, C.D., and Rakopoulos, D.C. (2008) Combustion and Performance Characteristics of a DI Diesel Engine Operating from Low to High Natural Gas Supplement Ratios at Various Operating Conditions, SAE Technical Paper, No. 2008-01-1392.
[6] Wannatong, K., Akarapanjavit, N., Siangsanorh, S., and Chanchaona, S. (2007) Combustion and Knock Characteristics of Natural Gas Diesel Dual Fuel Engine, SAE Technical Paper, No. 2007-01-2047.
[7] Aroonsrisopon, T., Salad, M., Wirojsakunchai, E., Wannatong, K., Siangsanorh, S., and Akarapanjavit, N. (2009) Injection Strategies for Operational Improvement of Diesel Dual Fuel Engines under Low Load Conditions, SAE Technical Paper, No. 2009-01-1855.
[8] Hsu, B.D. (2002) Practical Diesel-Engine Combustion Analysis, SAE International.
[9] Tepimonrat, T., Kamsinla, K., Wirojsakunchai, E., Aroonsrisopon, T., and Wannatong, K. (2011) Use of Exhaust Valve Timing Advance for High Natural Gas Utilization in Low-Load Diesel Dual Fuel Operation, SAE Technical Paper, No. 2011-01-1767.
[10] Czerwinski, J., Comte, P., Zimmerli, Y. (2003) Investigations of the Gas Injection System on a HD-CNG-Engine, SAE Technical Paper, No. 2003-01-0625.
[11] Wattanapanichaporn, O., Jantaradach, W., Wannatong, K., and Aroonsrisopon, T., (2012) Cylinder-to-Cylinder Variations in Diesel Dual Fuel Combustion under Low-load Conditions, submitted to the 26th Conference of the Mechanical Engineering Network of Thailand (ME-NETT 26).
[12] Pattarajaree, E. (2011). A Numerical Study of Intake Flow Phenomena in Diesel Dual Fuel Engine, M.Eng. Thesis, Kasetsart University.

7. Abbreviations

aBDC	After bottom dead center
aTDC	After top dead center
bBDC	Before bottom dead center
bTDC	Before top dead center
CFD	Computational fluid dynamics
CH_4	Methane
CO	Carbon monoxide
COV	Coefficient of variation
Cyl 1	Cylinder 1
Cyl 2	Cylinder 2
Cyl 3	Cylinder 3
Cyl 4	Cylinder 4
DDF	Diesel dual fuel
DOHC	Double overhead camshaft
EGR	Exhaust gas recirculation
EOI	End of injection timing
HC	Hydrocarbon
HRR	Heat release rate
IMEPn	Net indicated mean effective pressure
IVC	Intak valve close
IVO	Intake valve open
LHV	Lower heating value
NEDC	New European Driving Cycle
NO_X	Nitrogen oxide
TDC	Top dead center
THC	Total hydrocarbon